25th ABCM International Congress of Mechanical Engineering
October 20-25, 2019, Uberlândia, MG, Brazil

COB-2019-0402
PRELIMINARY INVESTIGATIONS OF THE GAS PROPERTY EFFECTS ON THE COOLING PARAMETERS

Janaina Ferreira da Silva
janaina.fs.eng@gmail.com
Ana Adalgiza Garcia Maia
anamaia@ita.br
Cleverson Bringhenti
cleverson@ita.br
Jesuino Takachi Tomita
jtakachi@ita.br
Aeronautics Institute of Technology (ITA)
Praça Marechal Eduardo Gomes, 50 - Vila das Acácias
São José dos Campos - São Paulo, Brazil

Abstract. *Substantial performance improvements might be achieved by increasing Turbine Inlet Temperature (TIT). However, this raises the heat load in turbine components requiring cooling to ensure safe operation and satisfy the performance and service time requirements. Many factors influence the required cooling airflow, such as the coolant and gas properties. Since some industrial engines may operate using more than one fuel type, it is of interest to investigate the effects of change the gas composition on the cooling parameters. In the present work, an in-house code estimates the cooling air parameters using the method described by Consonni. The fluid property calculation applies the two-component model. The fuels considered are kerosene (Jet-A); diesel; natural gas (pure methane); and, residual oil. Results showed a marked effect of the specific heat ratio c_{pc}/c_{pg} (i.e. air to gas ratio) on the coolant air fraction for the primary fuels, while other gas properties might become significant for non-conventional coolant and working fluid. The results highlight the importance of a detailed investigation of gas property effects on turbine cooling parameters.*

Keywords: *Gas Turbine, Turbine, Blade cooling, Flow properties, Fuel*

1. INTRODUCTION

Increasing Turbine Inlet Temperature (TIT) is one of the means to improve the performance for both aircraft and land-based gas turbines. However, environmental issues and material life requirements impose a limit on the rise of TIT. In modern gas turbines, TIT exceeds the maximum allowed temperature of the blade material. Cooling the components warrant safe operation while fulfilling performance and service time requirements. Nevertheless, the benefits brought about by higher TIT's are reduced by the losses associated with the turbine cooling system (Horlock *et al.*, 2001; Silva *et al.*, 2019). Higher the cooling air mass flow higher the pressure loss and lower the mainstream flow temperature.

The composition and properties of gas also affect engine performance. The combustion products depend on the fuel-air ratio, fuel chemistry, temperature, and pressure (Walsh and Fletcher, 2004; Guha, 2001). Since some industrial engines may operate using more than one fuel type, it is interesting to investigate the effect of these modifications. A hydrocarbon fuel burnt in the air mainly results in N_2, O_2, CO_2, and H_2O. Figures 1 and 2 show the variation of properties with the temperature for individual gas species. The water vapor content has a notable contribution to the specific heat at constant pressure (c_p), Fig. 1, and thermal conductivity (k), Fig. 2 (a). For all components, the dynamic viscosity (μ) exhibits similar variation at magnitude and temperature, as shown in Fig. 2 (b).

Carcasci *et al.* (2002) demonstrated that the mass flow composition affects the cooling performance. The authors analyzed some cooling parameters using alternative coolant and working fluids. The simulations maintained the maximum cycle temperature, coolant mass flow, blade and cooling system geometry fixed. According to the results, the composition of fluid affects the heat transfer coefficients changing the blade temperature distribution and hampering the blade cooling. Consequently, a reduction of maximum cycle temperature, redesign of the cooling system, or increasing the coolant mass flow could be required. All these conditions may lead to a decrease in engine performance. The analysis carried out in the present paper considers fixed the blade and cooling system geometry, imposing the same coolant fluid and blade metal temperature for all simulations. The purpose is to analyze the influence of gas mainstream properties on cooling performance parameters, paying attention to the effects on the coolant mass flow rate.

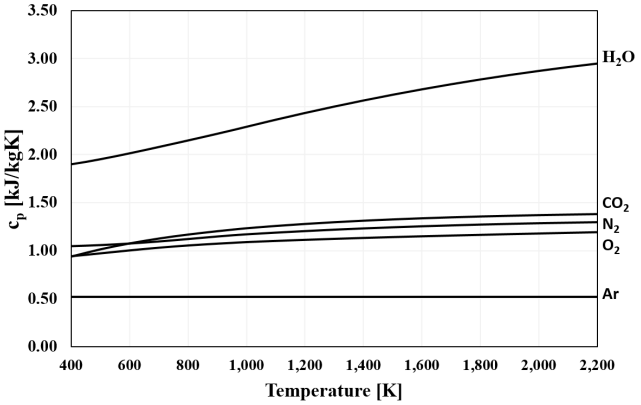

Figure 1: Variation of c_p versus temperature for individual species of the combustion products.

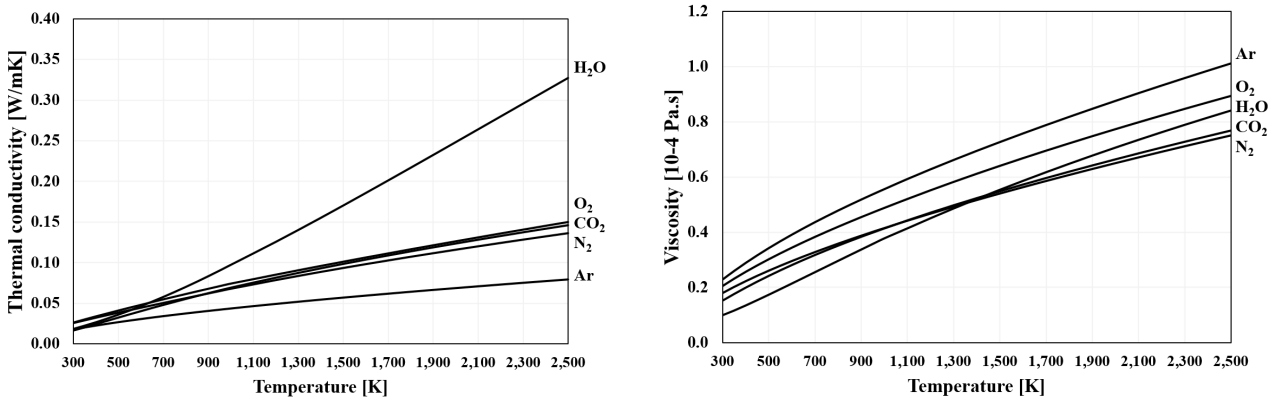

(a) Thermal conductivity k (b) Dynamic viscosity μ

Figure 2: Transport property variation versus temperature for individual species of the combustion products.

2. FLUID PROPERTIES

Since this work is a preliminary investigation about the gas property effects and to avoid additional complexity, the following approaches are adopted:

- The gas (combustion products) is assumed a mixture of its component species: Ar, N_2, O_2, CO_2, and H_2O (Wu, 1958), except for residual oil case;
- The effect of dissociation is negligible, even at elevated gas temperature;
- All properties are assumed to be dependent on temperature only;
- The flow properties are evaluated by considering the fluid composition as just air or gas (Young and Wilcock, 2002). Subscript c is appended to denote *coolant* (air) and g to denote mainstream *gas* (combustion products).

2.1 Cooling Fluid

The coolant flow composition affects cooling performance; as demonstrated by Carcasci *et al.* (2002) and Jordal *et al.* (2001). However, in this paper, the analysis is concerned with the influence of changing the hot gas composition. Then, only air is considered as coolant fluid in the simulations. The transport and thermodynamic properties of air are based on reported data by Green and Maloney (1997).

2.2 Fuels

Gas turbines may operate with different fuels depending on application. For example, kerosene is almost exclusively used for aero-engines, diesel for marine engines, and natural gas for land-based power generation engines. Industrial engines may also operate on more than one fuel type and with alternative fuels (Deuker *et al.*, 2001; Molière and Pommel, 2000).

In the present analysis, three fuels have been considered: kerosene (Jet-A); diesel; and natural gas (pure methane). These fuels comprise a mixture of many chemical compounds; nevertheless, to simplify the calculations, the approximated

compositions given in Tab. 1 are adopted. The pure methane CH_4 is the reference case. Simulations have also performed with residual oil that on a molar basis is 44.65% N_2, 22.10% CO, 21.17% CO_2, 7.24% H_2O, 4.83% H_2 and 0.01% H_2S.

Table 1: Fuel composition and Low Heating Value (LHV) (Elgohary and Seddiek, 2012; Air BP, 2011; Consonni, 1992)

Fuel	Molecular Formula	LHV [kJ/kg]
Jet-A	$C_{12}H_{23}$	43,020
Diesel	$C_{12}H_{26}$	42,800
Methane	C_1H_4	50,000

2.3 Combustion Products

The combustion of a given fuel with air results in a gas composition significantly different from working fluid before the combustion. The degree of change depends on both fuel to air ratio (FAR) and fuel composition (Walsh and Fletcher, 2004). It is therefore essential to take into account these gas properties in calculations to increase the accuracy of the results. There are several ways to evaluate these properties as briefly described below (Guha, 2001):

- *Method based on specified values:* Constant, standard values of properties are used in the estimations. For example, for preliminary cycle calculation, $c_p = 1,005\ kJ/kgK$ and $\gamma = 1.4$ (ratio of specific heats) are assumed for the compression process (air) and $c_p = 1,157\ kJ/kgK$ and $\gamma = 1.33$ are assumed for the expansion process (combustion gases) (Walsh and Fletcher, 2004). Values based on a mean temperature within each process are also used;

- *Method of using empirical relations:* When the fuel has a relatively fixed composition (e.g. kerosene), the properties of their combustion products can be determined by specific formulae that depend on temperature and fuel-air ratios alone (Walsh and Fletcher, 2004);

- *Method of using property tables:* The properties of the combustion products are presented as tabular data sets for selected values of temperature and actual fuel-air ratios (Kennan and Kaye, 1948) or calculated from tabulated values for air and stoichiometric fuel-air ratio properties (Wu, 1958);

- *Method based on gas composition:* In this approach the composition of the combustion products must be known. Hence, the properties of each constituent gas are calculated and combined to give the respective value for the mixture. This approach is adopted here.

The thermodynamic and transport properties of each gas component species are estimated from functions reported by McBride *et al.* (1993); without considering the equilibrium reaction contribution and dissociation. Table. 2 presents the equations; the constants a, A, b, B, C, D are quoted in the reference (McBride *et al.*, 1993). These equations were implemented into an in-house code to working fluid property evaluations. Figures 1 - 2 show the properties of some gases calculated by the program.

Table 2: Thermodynamic and transport equations (McBride *et al.*, 1993).

Description	Equation
Heat capacity	$\frac{c^0{}_p(T)}{R} = \sum_{i=1}^{n} \mathbf{a_i} T^{i-1}$
Enthalpy	$\frac{H^0(T)}{RT} = \frac{b_1}{T} + \frac{\int c^0{}_p(T)dT}{RT}$
Entropy	$\frac{S^0(T)}{R} = b_2 + \int \left(\frac{c^0{}_p(T)}{RT}\right) dT$
Viscosity Thermal conductivity	$\left.\begin{matrix}\ln \mu \\ \ln k\end{matrix}\right\} = AlnT + \frac{B}{T} + \frac{C}{T^2} + D$

Knowing the molar fraction y and the thermodynamic properties (i.e $c_{p,g}$, enthalpy h_g, entropy s_g) of the individual species; the respective property values for the combustion products can be evaluated (Walsh and Fletcher, 2004; Guha, 2001). For transport properties, once the dynamic viscosity μ_i of the component species has been determined, μ_g of combustion products is calculated according to the mixture formulation reported by Wilke (1950),

$$\mu_g = \sum_i \left\{ (\mathbf{y_i}\mu_\mathbf{i}) / \left[\mathbf{y_i} + \sum_j (\mathbf{y_j}\mathbf{\Phi_{ij}}) \right] \right\}, \tag{1}$$

where, *i* and *j* are the pure component of mixture. Φ_{ij} is the viscosity interaction coefficient between species *i* and *j* defined by:

$$\mathbf{\Phi_{ij}} = \left(1/\sqrt{8}\right) (1 + \mathbf{M_i}/\mathbf{M_j})^{-1/2} \left[1 + (\mu_\mathbf{i}/\mu_\mathbf{j})^{1/2} (\mathbf{M_j}/\mathbf{M_i})^{1/4}\right]^2. \tag{2}$$

where M is the molecular weight of components.

The approach given by Gordon and McBride (1994) is used to evaluate the thermal conductivity k of the combustion products. The mixture method has the form of Eq. (1), with μ and Φ_{ij} replaced by k and Ψ_{ij}, respectively. Ψ_{ij} is the frozen thermal conductivity interaction coefficient between species i and j,

$$\mathbf{\Psi_{ij}} = \mathbf{\Phi_{ij}} \left[1 + \frac{2.41(\mathbf{M_i} - \mathbf{M_j})(\mathbf{M_i} - 0.142\mathbf{M_j})}{(\mathbf{M_i} + \mathbf{M_j})^2}\right]. \tag{3}$$

Once c_p, μ and k are known, the Prandtl number (Pr) can be calculated:

$$Pr = \frac{c_p \mu}{k}. \tag{4}$$

3. COOLING PREDICTIONS

The coolant mass flow and other cooling influencing parameters are evaluated by an one-dimensional code based on the method described by Consonni (1992) and extended to be applied to the whole blade chord (Jordal *et al.*, 2001). This model considers in detail the blade geometry and allows to investigate the influence of fluid properties on cooling performance parameters.

Independently of the cooling technique used or if TBC (Thermal Barrier Coating) is presented, the following assumptions are considered:

- The inlet gas total temperature T_{0g} is constant in the spanwise and chordwise direction (Torbidoni, 2004);
- As a safety margin, the coolant estimation is based on the peak gas temperature given by $T_{gr,max} = T_{gr} + K_{comb}\Delta T_{comb}$, where T_{gr} is the gas recovery temperature, K_{comb} is the combustion pattern factor and ΔT_{comb} is the temperature rise through the combustor (Young and Wilcock, 2002);
- The coolant (T_{0c}) and blade metal (T_b) temperatures vary along the blade height (H_b) (Torbidoni, 2004);
- Blade metal temperature also varies through the blade walls and coating (Torbidoni, 2004).

3.1 Geometrical parameters

To avoid a large number of input data (mainly geometrical data) the internal blade geometry might be summarized by the value of cooling technology parameter Z (Consonni, 1992):

$$Z = \psi_i {\alpha_h}^{0.2} {n_p}^{0.8} E_h (c/d)^{1.2} \tag{5}$$

where, ψ_i is the coolant channel interference coefficient, α_h is the coolant passage cross-section/c^2, n_p is the number of internal passes of each coolant channel, E_h is the heat transfer augmentation factor, c is the blade chord and d is the cooling channel hydraulic diameter.

When set, this parameter allows to evaluate the influence of the internal blade geometry on blade cooling performance. The higher Z value, higher the cooling efficiency and coolant pressure drop and lower the required cooling mass flow (Torbidoni, 2004).

The external blade geometry is required to approximate the surface area exposed to the hot gas stream (gas side area); that is, the area to be cooled. The perimeter of blade S_g might be found from known the coordinate point of airfoil, Fig. 3; or assumed value of Φ_g, that $\Phi_g = S_g/c \geq 2$ (Torbidoni, 2004). Once the blade height is known the external blade area $A_{b,g}$ can be determined.

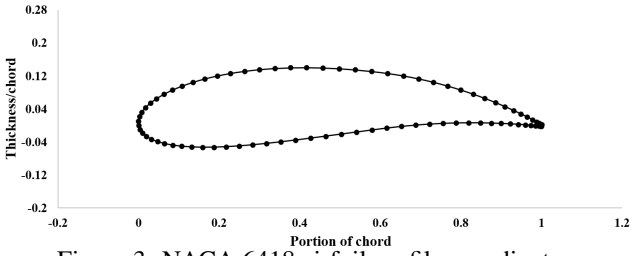

Figure 3: NACA 6418 airfoil profile coordinates.

3.2 Cooling parameter calculations

The convective cooling approach assumes that blade behaves like a cross-flow heat exchanger subjected to a hot gas flow with a thermal capacity much larger than the coolant flow (Consonni, 1992). The heat transfer is considered for an elementary area in the radial direction of the blade, Fig. 4. The equations expressing the heat transfer from gas to coolant are as follow:

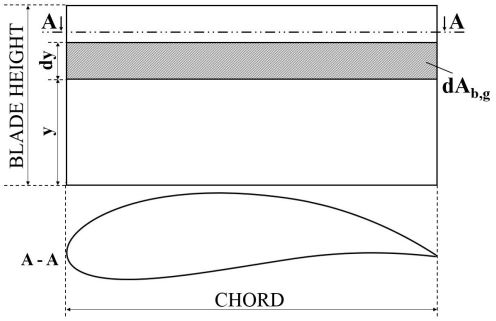

Figure 4: External elementary area $dA_{b,g}$ for heat transfer calculation.

$$d\dot{Q} = h_g dA_{b,g}(T_{gr} - T_{b,g}), \tag{6}$$

$$d\dot{Q} = \frac{k_b}{t_b} dA_{b,g}(T_{b,g} - T_{b,c}), \tag{7}$$

$$d\dot{Q} = h_c dA_{b,c}(T_{b,c} - T_{0c}), \tag{8}$$

$$d\dot{Q} = \frac{\dot{m}_c}{a_t z} c_{p,c} dT_{0c}. \tag{9}$$

where, h is the heat transfer coefficient, t_b is the thickness, a_t is the ratio between blades+shrouds surface and blade surface, z is the number of blades in each row.

Adding Eqns. (6-8) and that $a_c = dA_{b,c}/dA_{b,g}$ results:

$$d\dot{Q} = U_h dA_{b,c}(T_{gr} - T_{0c}), \tag{10}$$

where U_h is the overall coefficient of the heat transfer of the system,

$$U_h = \left[a_c \left(\frac{1}{h_g} + \frac{t_b}{k_b} \right) + \frac{1}{h_c} \right]^{-1}. \tag{11}$$

Equating the Eqns. (10) and (9):

$$\frac{\dot{m}_c}{a_t z} c_{p,c} dT_{0c} = -U_h dA_{b,c}(T_{gr} - T_{0c}). \tag{12}$$

Integrating this along the blade height, i.e. from $y = 0$ to $y = H_b$, and that $T_{0c}(0) = T_{0c,i}$ and $T_{0c}(H_b) = T_{0c,x}$, gives:

$$T_{gr} - T_{0c,x} = (T_{gr} - T_{0c,i}) e^{\frac{-\bar{U}_h A_{b,c}}{\left(\frac{\dot{m}_c}{a_t z}\right)\bar{c}_{p,c}}}. \tag{13}$$

Elaborating this last as regard to the cooling efficiency definition results:

$$\eta_c^{'} = \frac{T_{0c,x} - T_{0c,i}}{T_{gr} - T_{0c,i}} = 1 - e^{-NTU}, \tag{14}$$

$\eta_c^{'}$ is the cooling efficiency referring to the constant external gas temperature. NTU is the Number of Transfer Units,

$$NTU = \frac{\bar{U}_h A_{b,c}}{\left(\frac{\dot{m}_c}{a_t z}\right)\bar{c}_{p,c}}. \tag{15}$$

After elaboration (Torbidoni, 2004), NTU might be related to the coolant flow rate $\dot{m}_c$ as follows:

$$NTU = \frac{0.092 \frac{\bar{H}_b}{c} Z \left(\frac{\dot{m}_c}{\dot{m}_g}\right)^{-0.2}}{C_{g1}^{0.2} C_{f1} \left[1 + \left(a_c \frac{\bar{h_c}}{\bar{h_g}}\right)(1 + Bi_m)\right]}. \tag{16}$$

The coolant mass flow rate also affects the blade metal temperature. Then, it is necessary to derive the equation for the blade metal temperature. Equating the heat flux balance across the blade wall, Eqns. (6)-(8),

$$\frac{h_g}{a_c}(T_{gr} - T_{b,g}) = \frac{k_b}{t_b a_c}(T_{b,g} - T_{b,c}) = h_c(T_{b,c} - T_{0c}). \tag{17}$$

Dividing by h_c and $T_{b,max}$ and solving for blade metal temperature results,

$$\tau_{b,g} = \frac{\tau_{0c} + \left(Bi_m + \frac{\bar{h_g}}{a_c \bar{h_c}}\right)\tau_{gr}}{1 + Bi_m + \frac{\bar{h_g}}{a_c \bar{h_c}}}. \tag{18}$$

where τ is the non-dimensionalized temperature by the maximum permissible blade temperature $T_{b,max}$.

Figure 5 shows as the coolant flows from root to tip the coolant temperature increases. As consequence, it becomes less effective as a coolant, so that the blade temperature at the tip is higher than at the root. Assuming that T_{0g} is constant, the highest temperature on blade metal is located on both the external blade surface and the coolant exit section (Consonni, 1992; Chiesa and Macchi, 2004). Based on these assumptions and observing Eq. (14); Eq. (18) is rewritten for $\tau_{bg,out}$ - the actual maximum blade metal temperature:

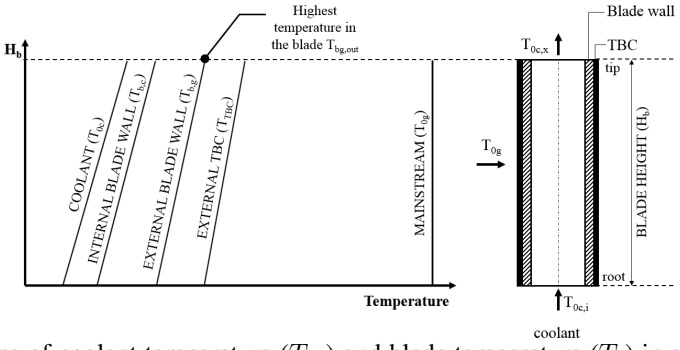

Figure 5: Spanwise variations of coolant temperature (T_{0c}) and blade temperature (T_b) in a blade with a single cooling channel.

$$\tau_{bg,out} = \frac{(1 - \eta_c^{'})\tau_{0c,in} + \left(\eta_c^{'} + Bi_m + \frac{\bar{h_g}}{a_c \bar{h_c}}\right)\tau_{gr}}{1 + Bi_m + \frac{\bar{h_g}}{a_c \bar{h_c}}}. \tag{19}$$

The equation system is complete. The main equations are summarized in Tab. 3. Details about the development of these equations are given in Consonni (1992) and Torbidoni (2004).

Table 3: Equation system of the model: Convective cooling (Torbidoni, 2004).

Description	Equation
Heat resistance ratio	$a_c \frac{\bar{h_c}}{h_g} = \frac{0.092 C_{g1}^{0.8} C_{f2} Z}{0.285 \Phi_g} \left(\frac{\dot{m}_c}{\dot{m}_g}\right)^{0.8}$
Number of Transfer Units	$NTU = \frac{0.092 \frac{\bar{H}_b}{c} Z \left(\frac{\dot{m}_c}{\dot{m}_g}\right)^{-0.2}}{C_{g1}^{0.2} C_{f1} \left[1+\left(a_c \frac{\bar{h_c}}{h_g}\right)(1+Bi_m)\right]}$
Cooling efficiency (T_{gr})	$\eta_c^{'} = \frac{T_{0c,x}-T_{0c,i}}{T_{gr}-T_{0c,i}} = 1 - e^{-NTU}$
Cooling efficiency ($T_{b,max}$)	$\eta_c = \frac{T_{0c,x}-T_{0c,i}}{T_{b,max}-T_{0c,i}} = \eta_c^{'} \left(\frac{T_{gr}-T_{0c,i}}{T_{b,max}-T_{0c,i}}\right)$
Non-dimensional blade metal temperature	$\tau_{bg,out} = \frac{(1-\eta_c^{'})\tau_{0c,in} + \left(\eta_c^{'} + Bi_m + \frac{\bar{h_g}}{a_c h_c}\right)\tau_{gr}}{1+Bi_m+\frac{\bar{h_g}}{a_c h_c}}$

Parameters C_{g1} and C_{f1} express the external blade geometry and the flow properties, respectively. C_{f2} is the second parameter related to the flow properties. They are defined as

$$C_{g1} = \frac{(H_b/c)}{a_t \sigma}, \tag{20}$$

$$C_{f1} = Pr_c^{2/3} \left[Re_g \cos\alpha_2 \left(\frac{\mu_g}{\mu_c}\right)\right]^{0.2}, \tag{21}$$

$$C_{f2} = Re_g^{0.17} \left(\frac{\bar{c}_{p,c}}{c_{p,g}}\right) \left(\frac{\mu_c}{\mu_g}\right)^{0.2} \left(\frac{Pr_g}{Pr_c}\right)^{2/3} (\cos\alpha_2)^{0.8}. \tag{22}$$

where α_2 is the gas flow angle at the exit row section, Re is the Reynolds number.

Given blade geometry, parameter Z, materials and estimated fluid properties, the cooling parameters and temperature profiles reported in Fig. 5 can be calculated. Since $\tau_{bg,out}$ is the maximum non-dimensional blade metal temperature, imposing the condition $\tau_{bg,out} = 1$ means that the blade metal temperature has an acceptable value in all the other blade sections, i.e. $T_{b,g} \leq T_{b,max}$ (Consonni, 1992). Therefore, to solve the equation system, an iterative process starts until the guessed values of $\dot{m}_c/\dot{m}_g$ satisfies the condition $\tau_{bg,out} = 1$.

As for convective cooling, the approach for film cooling is based on the relationship between the blade metal temperature $\tau_{bg,out}$ and the mass flow ratio $\dot{m}_c/\dot{m}_g$.

The adiabatic film effectiveness ϵ_f may be calculated by Eq. (23), which is derived from the semi-empirical correlation proposed by Goldstein and Haji-Sheikh (1967) and modified by Han and Jenkins (1982) - this correlation is based on the injection of the cooling air through a continuous slot over flat plates. Subscript inj refers to injection location.

$$\epsilon_f = 1.9 Pr_g^{2/3} \left\{1 + 0.329 \left(\frac{c_{p,g}}{c_{p,c}}\right) (Re_g)_{inj}^{0.8} \left(\frac{x}{c}\right)^{0.8} \left[2 a_t \sigma \left(\frac{\dot{m}_g}{\Delta \dot{m}_c}\right) \left(\frac{1}{r_{fc}}\right) \left(\frac{H_{inj} \pi D_m (\mu)_{inj}}{c \dot{m}_g}\right) + 0.00015 \frac{M_g}{M_c} \sin\alpha_{inj}\right]^{-1}. \tag{23}$$

where D_m is the blade row mean diameter, r_{fc} is the fraction of the coolant flow used for film cooling.

Using a similar procedure to that for convective model, the non-dimensional blade metal temperature may be derived:

$$\tau_{bg,out} = \frac{(1-\eta_c^{'})\tau_{0c,in} + \left(\eta_c^{'} + Bi_m + \frac{\bar{h_g}}{a_c h_c}\right)\tau_{aw}}{1 + Bi_{bw} + \frac{\bar{h_g}}{a_c h_c}}. \tag{24}$$

where τ_{aw} is the non-dimensionalized adiabatic wall temperature.

The mass flow ratio ($\dot{m}_c/\dot{m}_g$) is determined by means of an iterative calculation imposing the condition $\tau_{bg,out} = 1$.

The inclusion of TBC into the cooling model requires only accounts to the additional heat resistance representing the TBC layers.

4. RESULTS AND DISCUSSIONS

4.1 Comparison of cooling model results

The methodology described above was implemented into CTurb, an in-house code developed by Silva (2014), a program that is able to simulate turbine blade considering cooling. The simulation results were compared with data reported by Torbidoni (1999) to verify the accuracy, as shown in Figs. 6 – 8. The major input data are presented in Tab. 4.

Table 4: The main input data to verify the accuracy of predicting method (Torbidoni, 1999).

Geometrical parameters	H/D_m	0.1	c_x/D_m	0.6	t_b/c	0.125
	γ	65 deg	σ	1.2	Φ_g	2.6
Flow temperatures	$T_{0c,i}$	623 K	$T_{st,g}$	1,027 K	$T_{0,g}$	1,473 K
Flow parameters	Pr_g	0.74	Pr_c	0.7	Re_g	3.226x10^6
	μ_c/μ_g	0.8262	$c_{p,c}/c_{p,g}$	0.9142	Bi_{TBC}	0.0

In Figure 6 is shown the coolant flow rate $\dot{m}_c/\dot{m}_g$ versus parameter Z and portion of ejected coolant flow r_{fc}, where $r_{fc} = 0$ refers to convective blade cooling only and $r_{fc} = 1$ means that the all cooling flow is used to feed the film. The results from CTurb present good agreement with the reference data (Torbidoni, 1999). The cooling efficiency is shown in Figure 7. No marked difference between the results of CTurb and reference is observed. The adiabatic wall film effectiveness ϵ_f is showed in Figure 8 for calculated and reference data (Torbidoni, 1999). The results obtained are in good agreement with reference to all values of r_{fc} and parameter Z.

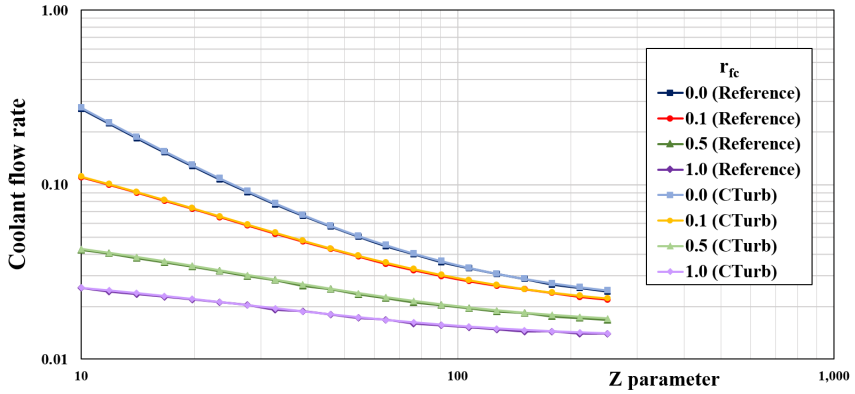

Figure 6: Coolant flow rate for film blade cooling. Plotted reference data are found in Torbidoni (1999).

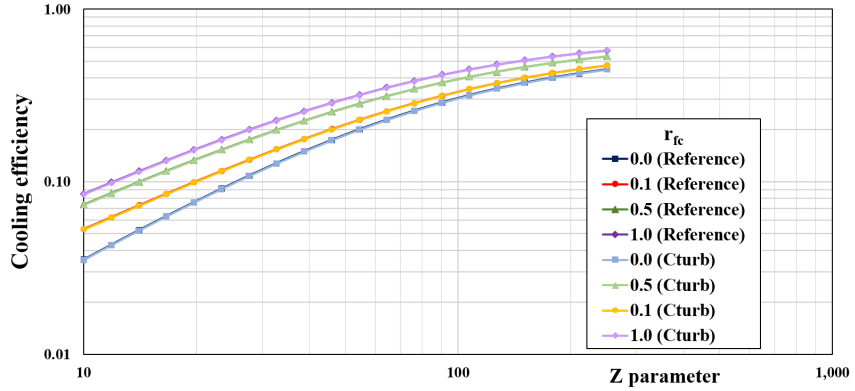

Figure 7: Cooling efficiency for film blade cooling. Plotted reference data are found in Torbidoni (1999).

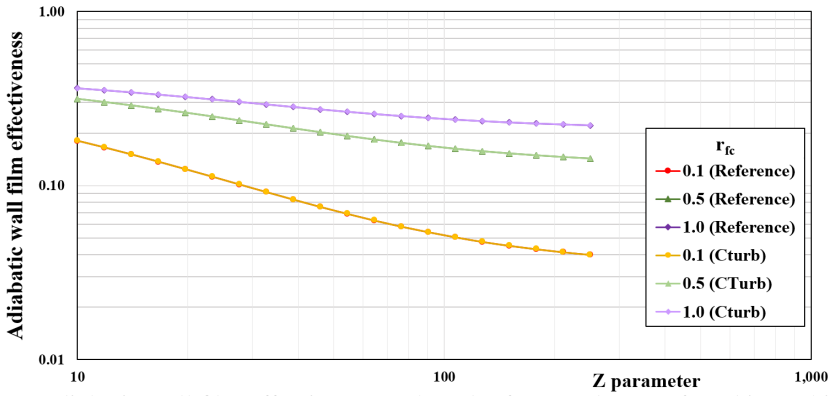

Figure 8: Mean adiabatic wall film effectiveness. Plotted reference data are found in Torbidoni (1999).

As conclusion, the implemented program demonstrated to predict correctly the cooling parameters with modifications in Z, r_{fc} and Bi_{TBC}. Then, the developed program might be used to simulate the engine with cooled blade turbine.

4.2 Cooled turbine blade simulation

For simulation of the cooled turbine blade the NACA 6418 profile was selected with 65 degree of stagger angle γ and 1.2 of solidity σ. The whole coolant flow feeds the film, i.e. $r_{fc} = 1.0$, which is injected at 25 degree (α_{inj}). The cooling technology parameter Z is 120 and metal Biot number $Bi_m = 0.5$, while $Bi_{TBC} = 0$. In addition, it follows that the maximum blade metal temperature is 1,075 K and the inlet coolant temperature is 643 K.

In order to better compare fuel composition effects, the same conditions were used in all simulations, including the geometrical parameters and cooling configuration, even though that in real engines some differences and limitations might exist. The objective is a direct comparison of the flow property effects in each case.

The presented results refer to a film-cooled nozzle with four rows of film injection holes. The relative distance from the injection location in the downstream chord-wise direction (x/c) was set at 0.25 (Torbidoni, 2004). As it is more usual, the notation expresses the coolant mass flow as a fraction of gas mass flow (i.e. $\dot{m}_c/\dot{m}_g$).

Figure 9 shows the cooling efficiency and adiabatic film effectiveness. The simulations were performed for kerosene (Jet-A), diesel and pure methane. From the results, it was observed that the gas composition almost does not affect the cooling parameters. While for the cooling flow rate $\dot{m}_c/\dot{m}_g$ a difference about 4% between CH_4 and kerosene at 1,800 K was found (see Fig. 10). In this case, the difference is due to the higher specific heat of gas resulting from the combustion of methane, Fig. 11. The difference owing to the other properties was negligible.

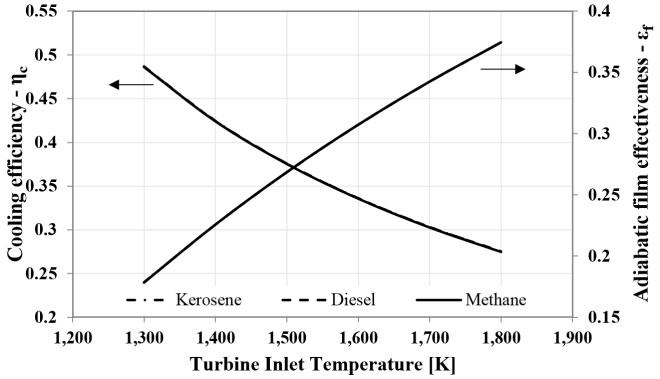

Figure 9: Cooling efficiency and adiabatic film effectiveness for different fuel compositions.

The effect of c_p is confirmed by the sensitivity study carried out to understand the relative impact of the flow properties in cooling parameters. The flow properties such as Pr_c and Re_g were varied over a range of 95-105 % of the nominal values for methane at TIT=1,400 K. Figures 12-14 show the effect of each flow parameter in the cooling variables ($\dot{m}_c/\dot{m}_g$, η_c and ϵ_f). A negative slope indicates that a lower cooling parameter is obtained by increasing the flow property.

In the range of investigated values, the parameter that has the largest impact on the coolant mass flow rate is $c_{p,c}/c_{p,g}$. Pr_g also shows a significant impact on the cooling variables, because the gas Prandtl number value affects the gas recovery temperature T_{gr}, C_{f2} and ϵ_f. For cooling efficiency only a smooth dependence was observed in coolant Prandtl number, about 1%. While for adiabatic film effectiveness, the changes were lower than 0.4%. Similar characteristics were obtained for the other fuels.

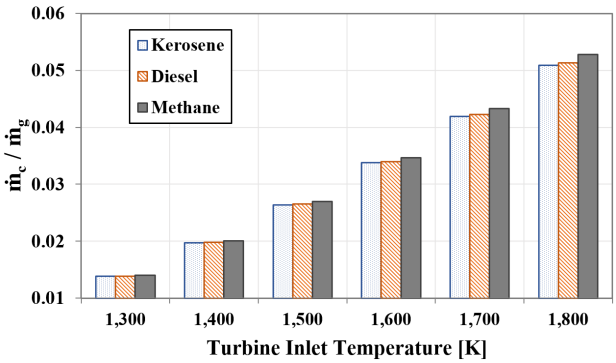

Figure 10: Cooling flow rate.

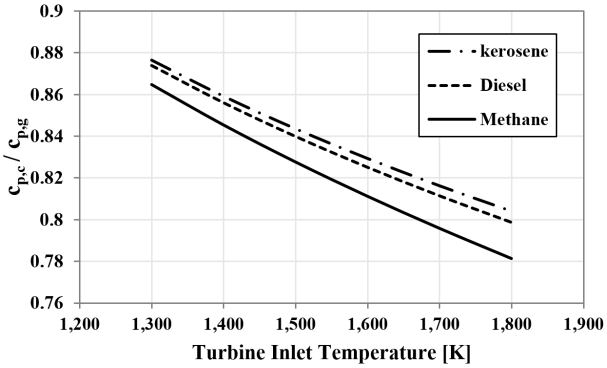

Figure 11: Specific heat coolant to gas ratio.

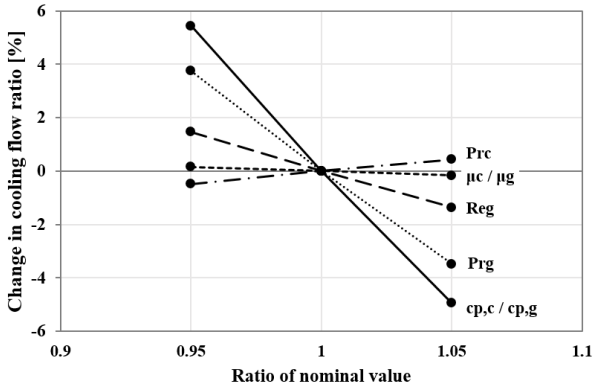

Figure 12: Impact of flow properties on the coolant mass flow rate.

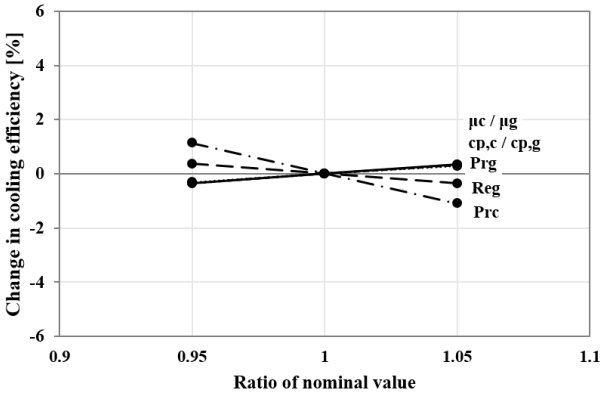

Figure 13: Impact of flow properties on the cooling efficiency.

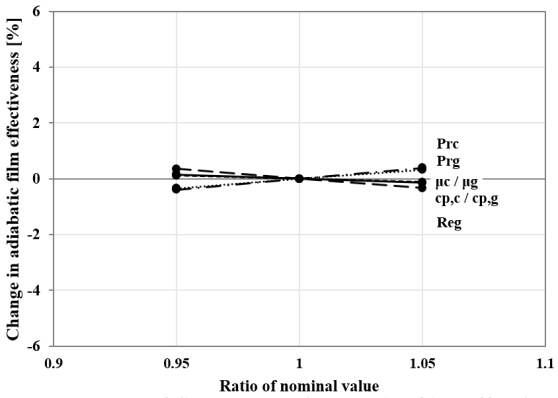

Figure 14: Impact of flow properties on the film effectiveness.

Simulations were also performed for residual oil fuel using CEA program (Gordon and McBride, 1994) for fluid property calculation. The results are compared with those from pure methane. The objective is to highlight the influence of fuel on cooling parameters once they present very different compositions. Figure 15 shows the cooling efficiency and adiabatic film effectiveness. A difference up to 5% and 3.4% was observed for η_c and ϵ_f, respectively. Higher differences were also observed for mass flow ratio, Fig. 16.

Analyzing the results of c_p, μ and Pr for both coolant and gas flow, the highest difference was 2.56% for Pr_g and less than 1% for the others. However, Reynolds number sharply increases for residual oil due to the higher FAR - which in turn increases $\dot{m}_g$, Fig. 17. From the sensitivity study (see Fig. 12), higher Reynolds number lower cooling flow ratio. Then, in this case, the Reynolds number had a relevant influence on the results. Besides, since the coolant mass flow is evaluated as a fraction of gas mass flow $\dot{m}_g$, the higher value of gas mass flow increases the coolant mass flow to be bled from mainstream flow as shown in Fig. 18.

It is recognized that considering film cooling for residual oil case should require a detailed investigation of the possibility of erosion/blockage of holes due to the fuel/air quality (Glezer, 2003). Nevertheless, the main goal is the direct comparison among the fuels and its influence on cooling parameters, hence this "real characteristic" has not been taken into account in the analysis.

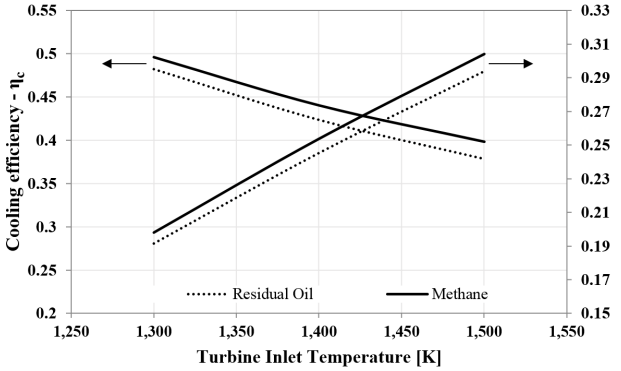

Figure 15: Cooling efficiency and adiabatic film effectiveness for methane and residual oil.

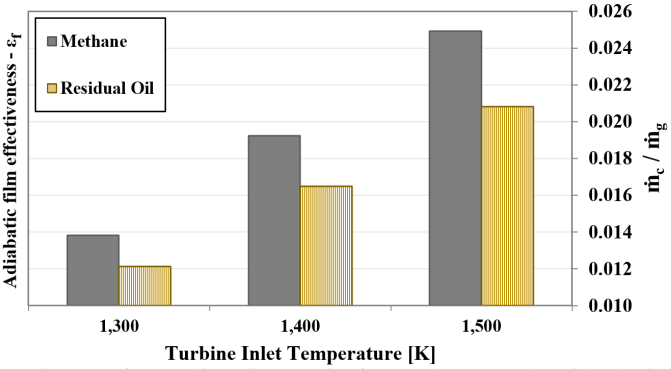

Figure 16: Cooling flow ratio for methane and residual oil.

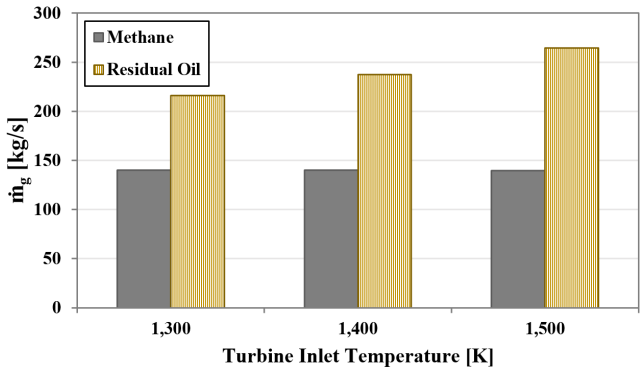

Figure 17: Mainstream gas mass flow.

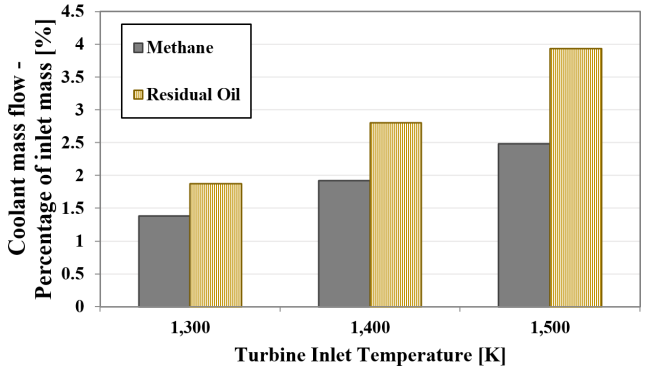

Figure 18: Bleed coolant mass flow for methane and residual oil.

5. CONCLUSIONS

In this paper, a film cooled nozzle was simulated using an in-house code developed for this purpose. The methodology proposed by Consonni (1992) was used to predict the cooling efficiency, film effectiveness, and mass flow ratio for different fuels. The objective of the study was to analyze and quantify the effects of gas composition on turbine cooling performance parameters.

The results did not demonstrate a marked difference in cooling efficiency and film effectiveness for the first three fuels investigated (kerosene, diesel, and methane). A difference of about 4% between CH_4 and kerosene was found for $\dot{m}_c/\dot{m}_g$, which for the reference fuel would represent an increase of 10 K in the external blade metal temperature. According to Han *et al.* (2000), this increase at the predicted blade temperature may reduce the blade life by approximately half. As demonstrated by the sensitivity study, $c_{p,g}$ has contributed to this difference, while the influence of other flow properties was negligible.

Higher differences were found for residual oil when compared to methane. In this case, the higher Reynolds number influenced the results, mainly the coolant and gas mass flow.

The present analysis highlights the importance of a detailed investigation of gas property effects on cooling parameters, which might become important mainly for non-conventional coolant and working fluid. Besides, the increase in blade metal temperature indicates a reduction in the blade creep life, but further analyses are required to quantify the level of degradation.

Finally, although the coolant considered was air, similar conclusions can be obtained for other coolant fluids keeping the same fuel; i.e., maintaining constant gas properties, because in the presented equations the flow properties might be represented as a fraction of gas or coolant.

6. ACKNOWLEDGEMENTS

CAPES (Coordenação de Aperfeiçoamento de Pessoal de Nível Superior), CNPq (Conselho Nacional de Desenvolvimento Científico e Tecnológico), FINEP (Financiadora de Estudos e Projetos) and FAPESP (Fundação de Amparo à Pesquisa do Estado de São Paulo) are acknowledged for their support to the research carried out at the Turbomachines Departament at ITA (Instituto Tecnológico de Aeronáutica).

7. REFERENCES

Air BP, 2011. "Handbook of products". Wayback Machine. Access 27 Sept. 2018 <https://web.archive.org/web/20120424223833/http://www.bp.com/subsection.do?categoryId=4503690contentId=7018443>.

Carcasci, C., Zecchi, S. and Oteri, G., eds., 2002. *Comparison of blade cooling performance using alternative fluids*, Vol. 2 of *Proceedings of ASME Turbo Expo 2002*. ASME. GT2002-30551.

Chiesa, P. and Macchi, E., 2004. "A thermodynamic analysis of different options to break 60% eletric efficiency in combined cycle power plants". *Journal of Engineering for Gas Turbine and Power*, Vol. 126, No. 4, pp. 770–785.

Consonni, S., 1992. *Performance Prediction of Gas/Steam Cycles for Power generation*. Ph.D. thesis, Princeton University, Princeton.

Deuker, E., Waldinger, R., Rauh, H.U. and Schade, F., eds., 2001. *Multi Fuel Concept of the Siemens 3A - Gas Turbine Series*, Vol. 2 of *Proceedings of ASME Turbo Expo 2001*. ASME. GT2001-0078.

Elgohary, M.M. and Seddiek, I.S., 2012. "Comparison between natural gas and diesel fuel oil onboard gas turbine powered ships". *Journal of King Abdulaziz University-Marine Science*, Vol. 23, No. 2, pp. 109–127.

Glezer, B., 2003. "Selection of a gas turbine cooling system". In E. Logan and R. Roy, eds., *Handbook of Turbomachinery*, Markel Dekker, Inc., New York, chapter 4, pp. 131–256. 2nd edition.

Goldstein, R.J. and Haji-Sheikh, A., eds., 1967. *Prediction of Film Cooling Effectiveness*, Proceedings of Semi-International Symposium. Japan Society of Mechanical Engineers.

Gordon, S. and McBride, B.J., 1994. "Computer program for calculation of complex chemical equilibrium compositions and applications. I. Analysis". Technical Report NASA RP-1311, NASA, Cleveland.

Green, D.W. and Maloney, J.O., 1997. *Perry's Chemical Engineer's Handbook*. McGraw-Hill chemical engineering series. McGraw-Hill, Singapore, 7th edition.

Guha, A., 2001. "An Efficient Generic Method for Calculating the Properties of Combustion Products". *Proc Instn Mech Engrs - Part A*, Vol. 215, No. 3, pp. 375–387.

Han, J.C. and Jenkins, P.E., 1982. "Prediction of film cooling effectiveness of steam". (ASME PAPER 82-GT-100).

Han, J.C., Dutta, S. and Ekkad, S., 2000. *Gas turbine heat transfer and cooling technology*. Taylor & Francis, New York.

Horlock, J.H., Watson, D.E. and Jones, T.V., 2001. "Limitations on Gas Turbine Performance Imposed by Large Turbine Cooling Flows". *Journal of Engineering for Gas Turbines and Power*, Vol. 123, No. 3, pp. 487–494.

Jordal, K., Torbidoni, L. and Massardo, A.F., eds., 2001. *Convective Blade Cooling Modelling for the Analysis of Innovative Gas Turbine Cycles*, Vol. 2 of *Proceedings of ASME Turbo Expo 2001*. ASME. GT2001-0390.

Kennan, J.H. and Kaye, J., 1948. *Gas Tables*. Wiley, New York.

McBride, B.J., Gordon, S. and Reno, M.A., 1993. "Coefficients for calculating thermodynamic and transport properties of individual species". Technical Memorandum NASA TM-4513, NASA, Cleveland.

Molière, M. and Pommel, F., eds., 2000. *Alternative Fuels in Gas Turbine Applications: A Simple Method for Assessing the Influence of Fuel on Performances*, Vol. 2 of *Proceedings of ASME Turbo Expo 2000*. ASME. GT2000-0139.

Silva, J.F., 2014. "Desenvolvimento de ferramenta computacional para avaliar o desempenho de turbinas a gás com resfriamento". Master thesis, Instituto Tecnológico de Aeronáutica , São José dos Campos, Brazil.

Silva, J.F., Maia, A.A.G., Bringhenti, C. and Tomita, J.T., 2019. "An overview of blade cooling effects on turbine performance". In *Proceedings of 25rd International Congress of Mechanical Engineering - COBEM 2019*. Uberlândia, Brazil (paper submitted to COBEM 2019).

Torbidoni, L., 1999. "Development of a cooled gas turbine stage". Master thesis, Università Degli Studi di Genova, Genova, Italy.

Torbidoni, L., 2004. *A New Method to Evaluate the Performance of a High Temperature Gas Turbine Stage*. Ph.D. thesis, Università Degli Studi di Genova, Genova.

Walsh, P.P. and Fletcher, P., 2004. *Gas Turbine Performance*. Blackwell, Oxford, 2nd edition.

Wilke, C.R., 1950. "A viscosity equation for gas mixtures". *The Journal of Chemical Physics*, Vol. 18, No. 4, pp. 517–519.

Wu, C.H., 1958. *Tables of Thermodynamic Properties of Combustion Gases*. Science Press, Peking.

Young, J.B. and Wilcock, R.C., 2002. "Modeling the air-cooled gas turbine. Part 1 – general thermodynamics". *Journal of Turbomachinery*, Vol. 124, No. 2, pp. 207–213.

8. RESPONSIBILITY NOTICE

The authors are the only responsible for the printed material included in this paper.